



Published in final edited form as:

Cytoskeleton (Hoboken). 2012 December ; 69(12): 1069–1085. doi:10.1002/cm.21077.

Targeted proteomic dissection of *Toxoplasma* cytoskeleton sub-compartments using MORN1

Alexander Lorestani¹, F. Douglas Ivey¹, Sivasakthivel Thirugnanam¹, Michele A. Busby¹, Gabor T. Marth¹, Iain M. Cheeseman², and Marc-Jan Gubbels^{1,*}

¹Boston College, Department of Biology, Chestnut Hill, MA 02467, USA

²Whitehead Institute for Biomedical Research, Department of Biology, Nine Cambridge Center, MA 02142, USA

Summary

The basal complex in *Toxoplasma* functions as the contractile ring in the cell division process. Basal complex contraction tapers the daughter cytoskeleton toward the basal end and is required for daughter segregation. We have previously shown that the protein MORN1 is essential for basal complex assembly and likely acts as a scaffolding protein. To further our understanding of the basal complex we combined subcellular fractionation with an affinity purification of the MORN1 complex and identified its protein composition. We identified two new components of the basal complex, one of which uniquely associated with the basal complex in mature parasites, the first of its kind. In addition, we identified several other novel cytoskeleton proteins with different spatiotemporal dynamics throughout cell division. Since many of these proteins are unique to Apicomplexa this study significantly contributes to the annotation of their unique cytoskeleton. Furthermore we show that G-actin binding protein TgCAP is localized at the apical cap region in intracellular parasites, but quickly re-distributes to a cytoplasmic localization pattern upon egress.

Keywords

Apicomplexa; *Toxoplasma*; MORN1; basal complex; cytoskeleton; motility; IMC

Introduction

The Apicomplexa comprise an extensive group of obligate intracellular parasites with complex life cycles across diverse host ranges (Keeling et al. 2005). These include several human parasites, with the malaria-causing *Plasmodium* genus being the most notorious member, next to the opportunistic parasites *Toxoplasma gondii*, causing encephalitis in immuno-compromised individuals as well as birth defects, and *Cryptosporidium* species, causing severe diarrhea. One of the defining features of the Apicomplexa is their cortical cytoskeleton, composed of flattened membrane sacs (alveoli), supported by a meshwork of intermediate filaments and microtubules (Leander and Keeling 2003; Morrissette and Sibley 2002). The cytoskeleton of Apicomplexa lies at the core of the biology of these organisms as it provides the platform for gliding motility (Baum et al. 2008), which is essential for host cell invasion, and in addition it serves as the scaffold for daughter cell assembly in cytokinesis (Striepen et al. 2007). The alveoli supported by the intermediate filaments are collectively known as the inner membrane complex or IMC (Mann and Beckers 2001). In

*corresponding author: gubbelsj@bc.edu.

The authors declare no conflict of interest.

Toxoplasma the most apical, cone-shaped alveolar vesicle defines the apical cap whereas three additional rows of multiple vesicles make up the rest of the parasite's IMC (Morrissette and Sibley 2002; Porchet and Torpier 1977). In recent years, the apical cap has gained interest as a distinct sub-domain of the IMC since a growing number of proteins is localizing distinctly to the cap, though the function of this organization is currently unclear (Anderson-White et al. 2011; Beck et al. 2010; Frenal et al. 2010; Gilk et al. 2006; Hu et al. 2006).

Parasite motility is provided by an actinomyosin-based process anchored in the IMC. Myosin A (MyoA) is part of the glideosome complex (Keeley and Soldati 2004), which further contains glideosome anchoring proteins GAP45 and GAP50 (Gaskins et al. 2004; Johnson et al. 2007), myosin light chain MLC1 (Herm-Gotz et al. 2002), and essential light chain ELC1 (Nebl et al. 2011). In the apical cap GAP70 replaces GAP45 in the glideosome (Frenal et al. 2010). MyoA transports actin filaments polymerizing in the space between the plasma membrane and the outer leaflet of the IMC. Actin in turn is anchored to adhesion proteins sticking through the plasma membrane that are in contact with extracellular substrate or receptors present on the host cell surface (Sibley 2004; Soldati and Meissner 2004). Actin in Apicomplexa is divergent from mammalian actin and can only form short, unstable filaments (Sahoo et al. 2006; Skillman et al. 2011; Wong et al. 2011). Furthermore, actin biology is characterized by a relatively limited set of actin binding protein proteins that control nucleation, stability, and turnover (Baum et al. 2006). In short, the behavior of actin and its interaction with the glideosome is not well understood and mechanisms appear to differ between parasites as well as between different life stages of the same parasite (e.g. (Daher et al. 2012; Daher et al. 2010; Ganter et al. 2009; Hliscs et al. 2010; Mehta and Sibley 2010; Skillman et al. 2012)). Moreover, *Toxoplasma* tachyzoites display several distinct modes of motility, including circular gliding, helical gliding, and twirling (Hakansson et al. 1999); most other parasites only display circular gliding (Sibley 2004). The mechanism and purpose of these different motility modes is presently unclear.

Apicomplexan parasites divide by a several different strategies that produce from 2 to 10,000s of daughter parasites per division round. A constant in these division processes is that daughter parasites are produced by budding, which is driven by assembly of the parasite's cortical cytoskeleton (Ferguson et al. 2008; Striepen et al. 2007). Daughter assembly starts with the apical end and progresses in the basal direction eventually resulting in contraction of the basal complex at the leading edge to taper the parasites toward the end. A ubiquitous factor is the presence of scaffolding protein MORN1 in the basal complex (Ferguson et al. 2008; Gubbels et al. 2006; Hu 2008; Hu et al. 2006). Apicomplexan cell division has been most extensively studied in *Toxoplasma gondii* tachyzoites, which produces two daughters per division round making it the simplest apicomplexan cytokinesis mode. In this system, ablation of MORN1 prevents assembly of the basal complex and results in conjoined parasite daughters, illustrating the basal complex provides the contractile power required to taper the cytoskeleton (Heaslip et al. 2010; Lorestani et al. 2010).

Next to MORN1, several other proteins have been shown to localize to the basal complex, including myosin C (Delbac et al. 2001), a dynein light chain (DLC1) (Hu et al. 2006), TgCentrin2 (Hu 2008), and several intermediate filament-like proteins of the IMC family (Anderson-White et al. 2011). However, only MORN1 is present at the leading edge throughout daughter assembly whereas the other components are recruited at the widest point. Which motor provides the power to contract the basal complex in the second half of cytoskeleton assembly is still not clear. A role for a myosin in cell division is questionable since actin polymerization does not appear to be required for cell division (Shaw et al. 2000) and MyoC is not conserved across the Apicomplexa, whereas DLC1 would require

microtubules, which are absent from the basal complex (Morrisette and Sibley 2002) although a form of deetyrosinated tubulin is present at the basal end (Xiao et al. 2010). Since Centrin2 is a contractile, filament forming protein it has been suggested as the most likely motor for contraction (Hu 2008). However, the role of TgCentrin2 in the basal complex, as well as other distinct locations in the cytoskeleton, is poorly understood (Hu et al. 2006). Furthermore, MORN1 is also present at the apical complex, the spindle pole, and the spindle, indicating it plays a versatile role in cell division (Gubbels et al. 2006). It is of note that genetic removal of MORN1 does not affect mitosis, but only interferes with basal complex assembly (Heaslip et al. 2010; Lorestani et al. 2010). Finally, the basal complex is maintained at the posterior end of mature parasites and likely serves a structural function (Anderson-White et al. 2011).

In this paper we set out to use MORN1 as a gateway to further dissect the basal complex. We isolated the putative MORN1 complex by a combination of cellular fractionation and immuno-precipitation and identified its components by mass spectrometry. We analyzed the list of candidates by their mRNA expression profiles throughout tachyzoite development and identified a pool of genes with mRNA expression profiles matching that of MORN1. We determined the sub-cellular localization patterns of the hypothetical proteins in this pool. We identified several new, previously uncharacterized proteins of the basal complex. In addition, we identified several other cytoskeleton proteins of which several specifically localized to the apical cap and others to the general cortical cytoskeleton. Overall, the results further our understanding of the composition and dynamics of the cytoskeleton throughout cell division.

Materials and Methods

Parasites

The type I strain RH and its transgenic derivatives were used throughout this study as described previously (Roos et al. 1994). In short, parasites were maintained by serial passage through human foreskin fibroblasts (HFFs), in DMEM supplemented with 1% fetal bovine serum, 50 units/mL penicillin, 50 ug/mL streptomycin 2 mM L-glut and 0.25 μ g/mL fungizone, at 37°C, 5% CO₂, and constant humidity. Stable transgenic parasite lines were selected by 20 μ M chloramphenicol or 1 μ M pyrimethamine, depending on the drug selection marker. All stable lines were cloned by limiting dilution.

Fractionation and Sample Preparation

RH strain parasites were harvested following natural egress, filtered (3 μ m), and washed twice in 1X PBS. The pellet was resuspended in lysis buffer (1% TX-100, 50 mM HEPES pH 7.5, 300 mM KCl, 1 mM EDTA, 1 mM MgCl₂, and 1X protease inhibitor), then mixed end-over-end for 1 hour at 4°C, and finally sonicated for three 30 second bursts (Cole Palmer Instrument Co. 4710 Series Ultrasonic Homogenizer set at 40% output control). The samples were spun at 14,000 \times g for 30 minutes at 4°C. The pellet was separated from the supernatant and resuspended in an equal volume of lysis buffer, and then fractionated over a 15–35% sucrose step gradient by centrifugation at 200,000 \times g for 18 hrs in a Ti-80 swinging bucket rotor. Samples were analyzed by silver staining and western blotting; the MORN1-enriched fractions were pooled and diluted 1:5 into binding buffer (50 mM HEPES pH 7.5 buffer containing 300 mM KCl) and pre-cleared over a column containing carbolinked pre-immune rabbit antiserum. The resulting flow-through fraction was then applied to a column containing carbolinked affinity-purified anti-MORN1 rabbit antiserum (Gubbels et al. 2006). The flow-through fraction was recycled once before washing the column in 30 bed volumes of 50 mM HEPES pH 7.5 buffer containing 300 mM KCl. α -MORN1 antibody-bound protein complexes were eluted using 200 mM glycine pH 2.5,

TCA-precipitated, washed, and dried in acetone prior to mass spectrometry analysis. Carbolinked antiserum columns were prepared using the CarboLink Immobilization Kit (Pierce/Thermo Scientific).

Mass spectrometry Analysis

Purified proteins were identified by mass spectrometry using an LTQ XL Ion trap mass spectrometer (Thermo Fisher Scientific) as described previously (Washburn et al. 2001) using reverse phase (C18) separation. Spectra were searched using SEQUEST software against ToxoDB's GT1, ME49 and VEG strains reference genomes.

Plasmids

All oligonucleotides used in this study are described in Supplementary Table S1. Endogenous Myc3x- and YFP-tagging constructs were engineered by LIC cloning 1.5 to 3.0 kb of the 3' genomic coding sequence, up to but not including the stop codon, into the pMyc-LIC-DHFR and pYFP-LIC-DHFR vectors (kind gift of Dr. Vern Carruthers, University of Michigan) (Huynh and Carruthers 2009). All other constructs were cloned based on the ptub-YFP₂(MCS)/sagCAT plasmid (Anderson-White et al. 2011) by replacing the α -tubulin promoter (*PmeI/BgIII*) with the endogenous promoter, or the first YFP (*BgIII/AvrII*) or the second YFP (*AvrII/EcoRV*) with the cDNA sequence of the gene of interest.

Sequence analysis

Sequences were collected from ToxoDB (www.toxoDB.org) (Gajria et al. 2008). Orthologs were detected using orthoMCL (Chen et al. 2006). Multiple sequence alignments were performed and color-coded using ClustalW2 (Goujon et al. 2010; Larkin et al. 2007). Palmitoylation sites were predicted using CSS-Palm 3.0 with a high threshold (Ren et al. 2008) and myristoylation sites were predicted by NMT Myr Predictor (<http://mendel.imp.ac.at/myristate/SUPLpredictor.htm>). Coiled-coils were predicted with the program COILS (Lupas et al. 1991). For genes of interest the mRNA expression profiles throughout tachyzoite development (Behnke et al. 2010) were downloaded from ToxoDB. Hierarchical clustering of gene expression profiles was performed in Matlab using the Spearman correlation as the distance metric.

Fluorescence microscopy

Extracellular parasite samples were prepared by settling freshly-lysed tachyzoites on poly-L-lysine-coated coverslips for 30 minutes and then washing the coverslips with 1X PBS. Intracellular parasite samples were prepared by infecting confluent monolayers of HFFs grown on coverslips with tachyzoites. All samples were fixed and permeabilized with either ice-cold 100% methanol or 3.7% paraformaldehyde and 0.25% Triton-X 100 and blocked in 1% BSA w/v in 1X PBS for 1 hour at room temperature. The following primary antibodies were used: rabbit anti-MORN1 (1:2000) (Gubbels et al. 2006), rat anti-IMC3 (1:2000) (Anderson-White et al. 2011), mouse anti-IMC1 (1:1000; kind gift of Dr. Gary Ward, University of Vermont) (Mann and Beckers 2001), mouse anti-c-myc (1:50; Santa Cruz Biotech), rabbit anti-GAP45 (1:2000; kind gift of Dr. Con Beckers, University of North Carolina) (Gaskins et al. 2004), rabbit anti-GFP (1:200; Torrey Pines Biolabs) mouse anti-GFP (1:500; Abgent). Alexa Fluor 488 and 594 goat anti-mouse, -rabbit and -rat secondary antibodies were used to probe the aforementioned primary antibodies (1:200, Invitrogen). 4',6'-diamidino-2-phenylindole (DAPI) was used to stain nuclear material. Images were collected using a Zeiss Axiovert 200M wide-field fluorescent microscope equipped with DAPI, FITC, YFP and TRITC filter sets, an a-Plan-Fluar 100X/1.45 NA oil objective and a Hamamatsu C4742-95 CCD camera. Images were collected, deconvolved and adjusted for phase-contrast using Volocity software (Improvision).

Detergent Extractions

Detergent extractions were performed as previously described (Gubbels et al. 2006). Essentially, 10^8 freshly-lysed tachyzoites were resuspended in 100 μ L of 10% detergent in resuspension buffer (150 nM NaCL, 50 mM Tris pH 7.5), or in resuspension buffer alone. Extraction with resuspension buffer, 1% TX-100 and 1% DOC were performed in ice for 1 hour, and with 1% SDS at 100°C for 10 minutes. The soluble and insoluble fractions were separated by centrifugation at 13,000 rpm for 20 minutes. Pellets were resuspended in 100 μ L resuspension buffer. 10 μ L of each fraction were run on a 12% Bis-Tris Gel and transferred to a PVDF membrane. Membranes were first probed with the following primary antibodies: mouse anti-c-myc-HRP (1:2000; Santa Cruz Biotech), mouse anti-IMC1 (1:1000), mouse anti-ISPI (1:2000; kind gift of Dr. Peter Bradley, UCLA), mouse anti-ROPI (1:1000) and mouse anti- α -tubulin 12G10 (1:1000; University of Iowa Hybridoma Bank). Primary antibodies not directly conjugated to HRP were detected by probing the membrane with goat anti-mouse-HRP (1:10000; DakoCytomation). Signals were collected by chemiluminescent substrate treatment (Advanta) and exposure to X-ray film.

Results

Proteomic dissection of the putative MORN1 complex

We isolated and enriched the putative MORN1 complex using the strategy depicted in Figure 1A. MORN1 associates with the parasite's cytoskeleton and is largely resistant to extraction in a 1% solution of the nonionic detergent Triton X-100 (TX-100) (Gubbels et al. 2006). Following TX-100 lysis of wild-type RH strain parasites and sonication, the insoluble pellet was fractionated on a 0–35% sucrose gradient. Silver stain analysis of the fractions confirmed the isolation of a complex and an abundant protein repertoire in each fraction (Fig 1B). Parallel western blot analysis of the fractions (Fig. 1C) identified fractions 3 and 4 as the most enriched in MORN1. To ascertain that this approach separated soluble and insoluble complexes, sucrose gradient fractions 3–5 of the TX-100 insoluble pellet and, as a control, fractions 3–5 of the TX-100 soluble supernatant separated on a parallel sucrose gradient, were separated on native blue gels and western blots probed with antibodies recognizing MORN1 (Fig. 1D), the insoluble inner membrane complex protein IMC1 (Fig. 1E) or the soluble microneme protein Mic2 (Fig. 1F). These data validated the separation of the parasite's TX-100 insoluble cytoskeletal components from the TX-100 soluble material. Additionally, the mass of the putative MORN1 complex isolated (Fig. 1D) appears to vary between 450–700 kDa, suggesting a variety of different compositions and/or complex fragments.

The MORN1-enriched fractions from the sucrose gradient (i.e. 3 and 4) were immunoprecipitated in two steps. The pooled gradient fractions were first pre-cleared with pre-immune IgG ("Carbo FT" in Fig. 1G and 1H) to eliminate non-specific background binding and subsequently immuno-affinity purified with anti-MORN1 IgG ("Carbo Elu" in Fig. 1G and 1H). As a negative control, a conditional MORN1 knockdown strain (MORN1-cKD, described in (Lorestani et al. 2010)) was grown in the presence of tetracycline for 72 hours to suppress transcription of MORN1 and then fractionated following the same protocol (Supplementary Figure S1). The purified MORN1 containing fractions and the corresponding MORN1-cKD control were subjected to mass spectrometry analysis. This identified 137 unique *Toxoplasma* proteins in the wild-type preparation (Supplementary Table S2). Only ten proteins were detected in the MORN1-cKD preparation, suggesting the enrichment of the putative MORN1 complex was very specific (Supplementary Table S3). The cohort identified in the wild-type preparation comprised 34 proteins with predicted functions in cellular metabolism (25% of total), 27 proteins with predicted functions in protein synthesis/modification/turnover (20% of total), 22 proteins secreted by the

micronemes, rhoptries or dense granules (16% of total), 20 hypothetical proteins (15% of total), 7 nuclear proteins (5% of total), 7 chaperones (5% of total), 5 associated with the actinomyosin motor (4% of total), 6 cytoskeletal proteins (4% of total), 4 mitochondrial proteins (3% of total), and 3 signaling proteins (2% of total).

Putative MORN1-complex proteins display different mRNA expression profiles

The set of 137 candidates identified by mass spectrometry was too large to be characterized in its entirety through experimentation. Furthermore, the diversity of putative functions was too great to establish a subset for further analysis *a priori*. Genome wide-transcriptome analysis throughout tachyzoite development has shown that genes with related functions, for instance genes encoding cytoskeletal components, display similar dynamics in their profiles (Anderson-White et al. 2011; Behnke et al. 2010). To curate an experimentally testable group of putative MORN1-interacting candidates, we hypothesized that most MORN1-interacting proteins would share mRNA expression profiles similar to that of MORN1.

Transcript expression profile data were available for 131 of the identified 137 proteins (95.6%). We used cluster analysis to identify a node that contained the candidates with mRNA expression patterns that appeared to peak during cytokinesis (Fig. 2A and Supplementary Figure S2). This group contains MORN1 and other confirmed cytoskeletal proteins (i.e. α - and β -tubulins, IMC4 and IMC10), several actinomyosin motor components (i.e. actin, ELC1, MyoA) and ten hypothetical proteins. The detection of cytoskeletal proteins with co-expressed transcripts was not surprising, as MORN1's association with this structure is well-established and the common role of these proteins in cytokinesis is generally accepted. The identification of actinomyosin motor components with co-expressed transcripts that peak during budding was unexpected because the proteins encoded by these transcripts are thought to play a role in extracellular, non-dividing parasites. Furthermore, most actinomyosin motor components only associate with the mature IMC (Gaskins et al. 2004). We did not further determine the specificity of the presence of actinomyosin motor complex proteins in the MORN1 fraction and therefore the ten hypothetical proteins in the prioritized list could be associated with either the putative MORN1 complex or actinomyosin motor complex.

Characterization of candidates

Based on the results of the cluster analysis thirteen genes were selected for further analysis (Table 1). The criteria we used are based on whether the gene has been characterized before, the gene's putative function, whether the gene's expression profile is related to MORN1, or whether it is related to the actinomyosin profile. Ten of the selected genes encode hypothetical proteins and were found in the node with MORN1 depicted in Figure 2A. A paralog (TGME49_002390) of one of these genes (TGME49_016650) was identified in a BLAST search against the *Toxoplasma* genome and selected for further investigation. A cyclase-associated protein, CAP (TGME49_110030), found in the node with MORN1 and a putative 14-3-3 protein (TMGE49_063090) found outside of the node with MORN1 were also followed up on because of their putative but unconfirmed roles in the actinomyosin complex.

Our primary evaluation criterion is whether the candidates co-localizes to one of the MORN1-containing structures. Hereto the coding sequences of the predicted open reading frames (ORFs) were PCR amplified and cloned into *Toxoplasma* expression vectors fused to YFP at either the N- or C-terminus. Eleven of the thirteen candidates were successfully cloned and expressed in *Toxoplasma*. The preliminary localization data are provided in Figure 2B and further detailed in Table 1. Candidates that appeared to localize to the cytoskeleton of intracellular parasites (TGME49_11338, TGME49_110030,

TGME49_016650, TGME49_002390, and TGME49_063090) were selected for further cell biological and biochemical analysis.

TgMSC1a (TGME49_016650) localizes to basal cup

The protein encoded by TGME49_016650 is predicted to be comprised of 436 amino acids and does not contain any detectable motifs. Orthologs were identified in *Neospora caninum* and *Plasmodium* spp. (Table 1). Additionally, a paralog was identified in *T. gondii* (TGME49_002390). Preliminary localization data (Fig. 2B) suggested that the overexpressed YFP fusion protein localized prominently to the basal complex, as well as to punctate structures along the periphery of the parasite and at the apical end of the parasite. We never observed an internal signal, indicating the protein does not associate with budding daughters but only with mature parasites.

To define the spatio-temporal localization pattern of the product of TGME49_016650, triple cMyc-epitope (Myc3x) and YFP tags were targeted to the 3' end of the endogenous locus of RHΔKu80 strain parasites (referred to as 016650-Myc3x and 016650-YFP henceforth). The localization of the tag in these parasites was similar to those overexpressing the exogenous YFP fusion protein. Localization to the basal cup was confirmed by co-staining methanol-fixed samples with MORN1 antiserum (Fig. 3A). 016650-YFP forms a ring structure (Fig. 3A lower inset) that is almost completely non-overlapping with the ring formed by MORN1 (Fig. 3A upper inset). Recently, we identified four distinct, partially overlapping sub-structures in the basal complex (Anderson-White et al. 2011). As such we probed whether this candidate co-localizes with any of the proteins marking these sub-structures. 016650-YFP cells co-stained with anti-IMC5 illustrated that 016650-YFP forms a ring around IMC5 (Supplementary Fig. S3A and S3B) and IMC8 (Supplementary Fig. S3C and S3D). MSC1a therefore did not co-localize with any known basal complex marker and adds another dimension to this complex structure.

Methanol fixation poorly preserves the cortical staining pattern observed in live parasites expressing 016650-YFP. Alternative fixation strategies were explored and fixation with 3.7% paraformaldehyde was found to preserve the cortical staining pattern at the expense of a well-preserved basal complex. Parasites fixed in 3.7% PFA were co-stained with anti-IMC3 to examine the localization of 016650-YFP throughout the cell cycle (Fig. 3B). This illustrated that 016650-YFP is absent from internal daughter buds and is deposited on parasites as they emerge from the mother. This makes this protein unique to the mature basal complex. The localization of 016650-YFP was unchanged in extracellular parasites (Fig. 3C).

The parasite's IMC protein meshwork and sub-pellicular microtubules are largely resistant to extraction with 1% non-ionic detergent TX-100 and ionic detergent deoxycholate (DOC). Differential detergent extractions were performed on 016650-Myc3x parasites to determine whether the protein is embedded in the mature IMC to which it localizes. 016650-Myc3x was completely solubilized by both 1% TX-100 and 1% DOC, as was ROP1, a soluble rhoptry protein used as a control (Fig. 3D). In support of this solubility is the presence of several putative palmytoylation sites (Cys10, 361, and 426). However, no myristoylation site could be identified, which is reminiscent of what is observed for ISP4 (Fung et al. 2012). Taking these data into account, we named the protein encoded by TGME49_016650 *Toxoplasma gondii* Mature Soluble Cytoskeletal protein 1a (TgMSC1a) and its paralog (TGME49_002390) TgMSC1b.

TgMSC1b (TGME49_002390) localizes to the mature IMC

TgMSC1b encodes a protein of 587 amino acids that shares 55% similarity and 36% identity to TgMSC1a. Orthologs were detected in *Neospora caninum* and *Plasmodium* spp. (Table 1). We chose to investigate this candidate because of its similarity to TgMSC1a, the similarity of its mRNA expression profile to the other candidate genes (i.e. peaks during budding), and preliminary localization data, which illustrated over-expressed TgMSC1b-YFP localizing to the cytoskeleton and to long fibers closely apposed to the cytoskeleton (Fig. 2B).

Like TgMSC1a, the over-expressed TgMSC1b-YFP was only observed in mature parasites. To elucidate the localization of this protein throughout the cell cycle, parasites expressing the TgMSC1b-YFP fusion under the control of the endogenous promoter were co-stained with the actinomyosin motor component GAP45 (Fig. 4A) and IMC1 (Fig. 4B). GAP45 is recycled from the mother parasite onto emerging daughters late in budding and marks the mature IMC (Gaskins et al. 2004; Gilk et al. 2009). Figure 4A shows parasites late endodyogeny when two daughters are emerging from each of the four mother parasites. GAP45 and TgMSC1b-YFP are only detectable in the mother's IMC and in the externalized components of the daughters. Probing the same parasites with anti-IMC1, which equally stains the mother and daughter IMC (Anderson-White et al. 2011; Mann and Beckers 2001), corroborate these data (Fig. 4B). The localization of TgMSC1b-YFP was unchanged in extracellular parasites (Fig. 4C).

To test whether this protein is embedded in the IMC, a strain wherein a Myc3x tag was attached the C-terminus of the endogenous locus was analyzed by differential detergent extraction. TgMSC1b-Myc3x was extracted with both 1% TX-100 and 1% DOC, and co-fractionated with the soluble control ROP1 (Fig. 4D). TgMSC1b contains one predicted palmytoylation site (Cys139) and no predicted myristoylation site that could potentially mediate membrane attachment. However, indirect cortical localization by binding to membrane-anchored proteins is also a possibility.

Tg14-3-3 (TGME49_063090) localizes to the centrosomes, daughter IMC, and basal cup

Across eukarya, 14-3-3 proteins form dimers and bind a wide spectrum of proteins involved in diverse cellular processes (Assossou et al. 2003). While 14-3-3 proteins have been identified in protozoan pathogens, little is known about their binding partners, cell biological function, or role in pathogenesis. Tg14-3-3 (TGME49_063090) is one of four 14-3-3 proteins encoded in the *Toxoplasma* genome and is widely conserved across the phylum. Particularly strong conservation in alpha helices 3, 5, 7 and 9, the interface of 14-3-3 proteins and their targets in other systems suggests a conserved substrate across the phylum (Supplementary Figure S4).

Tg14-3-3 was identified by mass spectrometry analysis of the putative MORN1 complex, however its mRNA expression profile did not cluster with that of MORN1. We chose to test this candidate experimentally because biochemical analysis of Tg14-3-3 suggested that, like MORN1, it was associated with both soluble and insoluble fractions of the parasite (Assossou et al. 2003). Furthermore, the over-expressed fusion protein localized prominently to the basal cup and to a peri-nuclear spot, in a manner similar to MORN1 (Fig. 2B).

Intracellular parasites expressing a Myc3x tag fused to the 3' end of the endogenous Tg14-3-3 allele were co-probed with anti-MORN1 (Fig. 5A). The colocalization of Tg14-3-3 with MORN1 in the basal cup is enlarged in the lower inset of Fig. 5A. The peri-nuclear 14-3-3 signal did not co-localize with MORN1 at the spindle pole (Fig. 5A upper inset). Instead, it appeared to localize in close apposition to the spindle pole suggestive of

co-localization with the centrosome. Co-staining with Centrin antiserum confirmed this observation and demonstrated the localization of Tg14-3-3 to the singular and duplicated centrosome(s) (Fig. 5B). To test whether the localization of this protein changed throughout cytokinesis, parasites were co-stained with anti-IMC3 and observed throughout budding (Fig. 5C and Supplementary Figure S5). Tg14-3-3 was detectable in the early daughter buds with IMC3 and remained associated with the daughter buds throughout budding. This localization pattern in dividing parasites is strikingly similar to that of IMC15 (Anderson-White et al. 2011). Surprisingly, in extracellular parasites most of the signal is cortical in a patchy pattern and cytoplasmic (Fig. 5D), as previously reported (Assossou et al. 2003). To determine whether this translocation was dependent upon MORN1, the localization of a 14-3-3 YFP fusion protein was characterized in MORN1-cKD parasites (Supplementary Figure S6). The localization of the fusion protein in intracellular parasites was found to be independent of expression of MORN1. We also tested Tg14-3-3 ionic detergent extractability and observed mostly soluble proteins next to a small insoluble fraction (Fig. 5E). Taken together, Tg14-3-3 co-localizes with MORN1 in the basal complex and is additionally present in the centrosomes, and in the cortical IMC, in particular in extracellular parasites. This suggests a complex and multifactorial role for Tg14-3-3.

TgILP1 (TGME49_113380) localizes to IMC

The protein product of TGME49_113380 is predicted to be 274 amino acids and is widely conserved across the Apicomplexa (Table 1). A coiled-coil domain spans amino acids 153 through 231. In all organisms this appears to be a single copy gene that is not part of a gene family.

Overexpression of the YFP fusion protein leads to grossly malformed cytoskeletons and large, irregular nuclei are often observed, suggestive of mitotic uncoupling (Supplementary Figure S7). The fusion protein localized to the mature malformed IMC, along with IMC3, as well as to small rings in the cytoplasm, independent of IMC3 (Supplementary Figure S7). In order to determine the physiological localization of this protein, parasites stably expressing a 113380-YFP gene controlled by the endogenous promoter were examined by fluorescence microscopy (Fig. 6A–C). The tagged protein localized to the mature IMC in intracellular (Fig. 6A) and extracellular parasites (Fig. 6C). In dividing parasites, the YFP-tagged protein was preferentially targeted to the daughter buds, as illustrated by co-staining with anti-IMC1, which stains mother and daughters evenly (Fig. 6B). This localization pattern has also been reported for IMC3, IMC10 (Anderson-White et al. 2011) and GAP50 (Frenal et al. 2010; Gaskins et al. 2004). Differential detergent extraction of parasites expressing a Myc3x tag fused to the 3' end of the endogenous locus revealed that 113380 is absolutely insoluble in both 1% TX-100 and 1% DOC solution, further supporting the characterization of this protein as an integral IMC component. However, this protein also contains multiple predicted palmitoylation sites (Cys95, 119, 250, 273, 274) that could additionally anchor this protein in the alveoli. Based on these insights, and the already long list of related IMC proteins containing alveolin domains (IMC1 and 3–15) as well as two phosphatases (IMC2a; TGGT1_083640 and IMC2b; TGGT1_083630), we named this protein IMC localizing protein 1 or ILP1 to clearly differentiate it from these families.

TgCAP (TGME49_110030) localizes to the apical cap

Cyclase-associated proteins (CAPs) are ubiquitous regulators of actin turnover that act through a conserved actin-binding domain (Hubberstey and Mottillo 2002). Analysis of the primary amino acid sequences of CAPs of several apicomplexan parasites, i.e. *T. gondii*, *C. parvum*, *P. falciparum* and *P. berghei*, revealed the absence of the adenylate cyclase binding domain for which the protein is named (Hliscs et al. 2010). The *C. parvum* CAP protein (XP_626004.1) is 45% identical and 62% similar to TgCAP and binds G-actin *in vitro*

(Hliscs et al. 2010). Reverse genetics has also shown that the CAP paralog in *P. berghei* is dispensable in the blood stage, but essential for oocyst development in the mosquito vector (Hliscs et al. 2010).

Where CAP proteins localize in apicomplexan parasites throughout the lytic cycle has thus far not been defined. The C-terminal YFP fusion protein driven by the tubulin promoter was targeted primarily to the apical cap, a sub-compartment of the parasite's cytoskeleton (Fig. 2B). A fluorescent spot was also observed in the parasite's cytoplasm, consistent with a previous report of discrete cytoplasmic bundles of actin (Dobrowolski et al. 1997). A parasite strain expressing TgCAP-YFP under the control of the endogenous promoter was probed with mAb 7E8, which specifically labels a component (ISP1) of the apical cap of mature and dividing parasites (Beck et al. 2010) (Fig. 7A). These data illustrate that in mature intracellular parasites, TgCAP is concentrated primarily in the apical cap and co-localizes with ISP1. TgCAP was to a lesser degree also detectable throughout the IMC. Co-staining with anti-IMC3 revealed that TgCAP is incorporated into the apical caps of daughter buds late in endodyogeny, prior to their emergence from the mother, reminiscent of the incorporation of RNG1 into the apical cap of mature daughter buds (Tran et al. 2010) (Fig. 7B and Supplementary Figure S8).

Outside of the host cell, the transient formation of short actin filaments between the parasite's plasma membrane and IMC is a critical event required for parasite motility. To test whether this G-actin sequestering protein translocates from the apical cap in intracellular parasites to another compartment in extracellular parasites, we co-stained extracellular TgCAP-YFP parasites with the ISP1 antibody (Fig. 7C). Under these conditions TgCAP, but not ISP1, translocated from the apical cap to the parasite's cytoplasm. Consistent with this transient localization pattern is the detergent soluble nature of TgCAP, which is performed on extracellular parasites (Fig. 7D).

Discussion

Proteomic approaches are well suited to addressing unknown aspects of cytoskeletal biology and have been used to characterize the proteomes of *Toxoplasma's* apical complex (Hu et al. 2006) and the pellicle of *Tetrahymena*, a related alveolar organism (Gould et al. 2011). In these studies parasites were fractionated by detergents and differential centrifugation to enrich the fraction of interest, and yielded hundreds of candidates for further experimental investigation. In another recent study immuno-precipitation was used to identify proteins associating with the IMC-associated protein GAP45 (Nebl et al. 2011), which provided another large inventory of proteins that may have a role in the cytoskeleton. In this study we aimed to define the composition of the basal complex using a combination of fractionation and immunoprecipitation of MORN1, its key scaffolding protein (Lorestani et al. 2010).

Of the 137 proteins that putatively associate with MORN1 we prioritized 13 candidates by selecting for transcription profiles similar to that of MORN1 as well as their functional annotation (Fig. 2A). Since nearly all the proteins we selected are hypothetical, with few known domain or functions, the first clue toward their function is provided by their sub-cellular localization pattern. Sub-cellular localization by YFP tagging identified two proteins that localize to the basal complex (Tg14-3-3 and TgMSC1a), two proteins that localize to the apical cap (TgCAP and TGME49_009600), and three proteins that localize more broadly to the IMC (TGME49_030160, TgMSC1b, and TgILP1). Besides the classification in these three groups, differences among the group members could be appreciated based on their specific spatiotemporal dynamics throughout the cell cycle, and their sensitivity to detergent extraction to assign their mode of cytoskeleton association.

The proteins excluded from our shortlist for follow up comprised many proteins unlikely to interact with MORN1 *in vivo* such as secreted and cytoplasmic proteins. Although western blot analysis of our MORN1 enriched fraction indicated the absence of microneme proteins (Fig. 1F), several proteins localizing to the secretory organelles were identified by mass spectrometry. Since these are absent from our MORN1-cKD negative control preparations the associations appear to be specific. However, one thing to keep in mind is that the putative function of MORN1 is a scaffolding protein. Consistent with such function is that it is likely sticky such that, following detergent lysis, certain organellar and cytoplasmic proteins formed aspecific yet strong interactions with MORN1. In essence, these data are consistent with a function of MORN1 in organizing protein-protein interactions and its hypothesized role as a scaffolding protein in assembling the basal complex (Lorestani et al. 2010).

We identified Tg14-3-3 and TgMSC1a as two new components localizing to the basal complex. In intracellular parasites Tg14-3-3 co-localizes with MORN1 in the basal complex, as well as to the centrosome throughout the cell cycle. However, in extracellular parasites Tg14-3-3 becomes cortical, localizing to the whole IMC. This translocation was further shown to be independent of MORN1. Since 14-3-3 proteins in many cases recognize phosphorylated sites in other proteins, this observation predicts a change in phosphorylation pattern of MORN1 e.g. when parasites egress from their host cell. Indeed there is evidence that MORN1 is phosphorylated (Treeck et al. 2011). Moreover, a role for 14-3-3 protein has been suggested in sequestering the inactive, phosphorylated form of the Actin Depolymerizing Factor (ADF) (Schuler and Matuschewski 2006). The translocation of Tg14-3-3 upon egress could therefore be consistent with a change in needs for G-actin sequestration and actin depolymerization (Allen et al. 1997; Mehta and Sibley 2010).

The other basal complex protein identified here, TgMSC1a, only localized to the basal complex in mature parasites and did not co-localize with any of the known basal complex sub-structures (Anderson-White et al. 2011). Our results (Supplementary Fig. S3) indicate that MSC1a resides in a structure flanked apically by MORN1, IMC9, and 13, while it flanks the IMC5 and 8 containing sub-structure laterally. This adds another distinct sub-structure in the basal complex (Anderson-White et al. 2011). The function of the basal complex in mature parasites is not well understood, however several clues are now accumulating. *Toxoplasma* encodes two related MSC genes, one localizing to the basal complex, and one localizing to the mature IMC. Only coccidia appear to have two genes, which is consistent with the presence of a basal complex across the zoites in these parasites e.g. as described for *Eimeria* (D'Haese et al. 1977). However, most apicomplexan zoites do not maintain a basal complex in mature parasites e.g. as observed in mature *Plasmodium* sporozoites (Kudryashev et al. 2010) and merozoites (Kono et al. 2012). The basal complex in mature *Toxoplasma* tachyzoites also contains Myosin C, a gene unique to *Toxoplasma* (Delbac et al. 2001), and a family of unique IMC proteins (Anderson-White et al. 2011). This might be why *Toxoplasma* harbors two MSC genes, one with a general cortical localization, anticipated to be conserved across the Apicomplexa, and one with a unique basal complex localization.

While we did identify two new proteins localizing to the basal complex, we did not find other components that were previously shown to localize to this structure, such as IMC5, 8, 9 and 13 (Anderson-White et al. 2011), TgDLC (Hu et al. 2006), Centrin2 (Hu 2008), or MyoC (Delbac et al. 2001). Earlier ultra-structural and immunofluorescence studies have illustrated that the basal complex is composed of multiple layers. The nature and strength of the interaction between these sub-compartments is unknown, hence the extraction conditions used in this study could have eliminated some of these interactions if they were weak. Moreover, our approach could therefore have prohibited the detection of additional, novel

basal complex proteins. In spite of this limitation, the 450–700 kDa size of the putative MORN1 complex on native blue gels (Fig. 2B) suggested the presence of different sized complexes, which is in line with the scaffolding function of MORN1. In future work we will therefore address the architecture of the basal complex by directed experiments using pull-down experiments with other basal complex components.

Of the three newly identified proteins that associate with the IMC, TgILP1 predominantly localizes to budding daughters, whereas TgMSC1b exclusively localizes to the mature IMC. The protein encoded by TGME49_030160 localizes to the daughter buds and mature IMC, but we have not yet characterized this protein in detail (results not shown). The spatio-temporal dynamics are consistent with different classes of IMC protein: TgILP1 with IMC3, 10 and TgMSC1b with IMC7, 12, 14. Therefore, our new data expand the insights on cytoskeletal proteins with distinct spatiotemporal signatures beyond the alveolin domain containing IMC proteins (Anderson-White et al. 2011).

Since MORN1 is also present in the apical complex, it is possible that we specifically identified some proteins residing on the apical end of the parasite. Of the two proteins localizing to the apical cap, TgCAP functions in G-actin sequestration (Hliscs et al. 2010). Interestingly, this specific localization is lost in extracellular tachyzoites and the signal becomes cytoplasmic. We did not observe such shift for other basal cap proteins such as IMC11 (Anderson-White et al. 2011), PhIL1 (Gilk et al. 2006) (data not shown) and ISP1 (Beck et al. 2010) whereas GAP70, the glideosome component specific for the apical cap, is needed in extracellular parasites to facilitate gliding (Frenal et al. 2010). It is unknown whether TgDLC (Hu et al. 2006) is released from the apical cap. TgCAP contains three predicted palmitoylation sites (Cys6, 8, 203) that could play a role in change in its localization dynamics, mediated by palmitoylation and depalmitoylation. However, more experiments are necessary to test this model. The presence of TgCAP in the apical cap fits a model wherein G-actin is sequestered at the site where gliding motility is needed first. Why it is being released after the parasites are gliding is less clear. In *Plasmodium* sporozoites a minor accumulation in the apical tip can also be appreciated but was not specifically reported (Hliscs et al. 2010). Our observation therefore provides a first potential clue toward a specific function of the apical cap. Whether the whole apical cap structure is present to support the sequestration of G-actin or otherwise has a specific function supporting the onset of gliding, which could be consistent with a specific glideosome component GAP70 localization to the cap, remains to be determined.

In addition to the novel cytoskeletal proteins and obvious aspecific binders, the status of several confirmed actinomyosin motility components (e.g. actin, ELC1, MyoA, profilin family protein, cyclase-associated protein, and aldolase) that were detected in the wild-type MORN1-enriched fractions but not in the control MORN1-cKD preparation is not as clear-cut. We can currently not exclude whether this interaction is aspecific or non-physiological, however the glideosome motor components are either embedded in or closely associated with the IMC, and as such a functional connection between the components of the motility apparatus and MORN1 can be envisioned.

Our findings are summarized in Figure 8. The collection of new cytoskeletal components is excitingly rich in proteins conserved across the Apicomplexa. This study therefore significantly contributes to the annotation of the apicomplexan cytoskeleton. Investigations into the localization and function of these proteins in other pathogens within the phylum will be important to understand the roles of these molecules in these organisms and will further contribute to understanding the biology of the unique apicomplexan cytoskeleton germane to motility and cell division.

Supplementary Material

Refer to Web version on PubMed Central for supplementary material.

Acknowledgments

We thank Con Beckers, Gary Ward, and Peter Bradley for generously sharing reagents. This work was supported by National Institutes of Health grants R01AI081924 and U54AI057159 through a New England Regional Center of Excellence in Biodefense and Emerging Infectious Disease developmental grant.

References

- Allen ML, Dobrowolski JM, Muller H, Sibley LD, Mansour TE. Cloning and characterization of actin depolymerizing factor from *Toxoplasma gondii*. *Mol Biochem Parasitol*. 1997; 88(1–2):43–52. [PubMed: 9274866]
- Anderson-White BR, Ivey FD, Cheng K, Szatanek T, Lorestani A, Beckers CJ, Ferguson DJ, Sahoo N, Gubbels MJ. A family of intermediate filament-like proteins is sequentially assembled into the cytoskeleton of *Toxoplasma gondii*. *Cell Microbiol*. 2011; 13(1):18–31. [PubMed: 20698859]
- Assossou O, Besson F, Rouault JP, Persat F, Brisson C, Duret L, Ferrandiz J, Mayencon M, Peyron F, Picot S. Subcellular localization of 14-3-3 proteins in *Toxoplasma gondii* tachyzoites and evidence for a lipid raft-associated form. *FEMS Microbiol Lett*. 2003; 224(2):161–8. [PubMed: 12892878]
- Baum J, Gilberger TW, Frischknecht F, Meissner M. Host-cell invasion by malaria parasites: insights from *Plasmodium* and *Toxoplasma*. *Trends Parasitol*. 2008; 24(12):557–63. [PubMed: 18835222]
- Baum J, Papenfuss AT, Baum B, Speed TP, Cowman AF. Regulation of apicomplexan actin-based motility. *Nat Rev Microbiol*. 2006; 4(8):621–8. [PubMed: 16845432]
- Beck JR, Rodriguez-Fernandez IA, Cruz de Leon J, Huynh MH, Carruthers VB, Morrisette NS, Bradley PJ. A novel family of *Toxoplasma* IMC proteins displays a hierarchical organization and functions in coordinating parasite division. *PLoS Pathog*. 2010; 6(9):e1001094. [PubMed: 20844581]
- Behnke MS, Wootton JC, Lehmann MM, Radke JB, Lucas O, Nawas J, Sibley LD, White MW. Coordinated Progression through Two Subtranscriptomes Underlies the Tachyzoite Cycle of *Toxoplasma gondii*. *PLoS ONE*. 2010; 5(8):e12354. [PubMed: 20865045]
- Chen F, Mackey AJ, Stoeckert CJ Jr, Roos DS. OrthoMCL-DB: querying a comprehensive multi-species collection of ortholog groups. *Nucleic Acids Res*. 2006; 34(Database issue):D363–8. [PubMed: 16381887]
- D'Haese J, Mehlhorn H, Peters W. Comparative electron microscope study of pellicular structures in coccidia (*Sarcocystis*, *Besnoitia* and *Eimeria*). *Int J Parasitol*. 1977; 7(6):505–18. [PubMed: 413801]
- Daher W, Klages N, Carlier MF, Soldati-Favre D. Molecular Characterization of *Toxoplasma gondii* Formin 3, an Actin Nucleator Dispensable for Tachyzoite Growth and Motility. *Eukaryot Cell*. 2012; 11(3):343–52. [PubMed: 22210829]
- Daher W, Plattner F, Carlier MF, Soldati-Favre D. Concerted action of two formins in gliding motility and host cell invasion by *Toxoplasma gondii*. *PLoS Pathog*. 2010; 6(10):e1001132. [PubMed: 20949068]
- Delbac F, Sanger A, Neuhaus EM, Stratmann R, Ajioka JW, Toursel C, Herm-Gotz A, Tomavo S, Soldati T, Soldati D. *Toxoplasma gondii* myosins B/C: one gene, two tails, two localizations, and a role in parasite division. *J Cell Biol*. 2001; 155(4):613–23. [PubMed: 11706051]
- Dobrowolski JM, Niesman IR, Sibley LD. Actin in the parasite *Toxoplasma gondii* is encoded by a single copy gene, ACT1 and exists primarily in a globular form. *Cell Motil Cytoskeleton*. 1997; 37(3):253–62. [PubMed: 9227855]
- Ferguson DJ, Sahoo N, Pinches RA, Bumstead JM, Tomley FM, Gubbels MJ. MORN1 has a conserved role in asexual and sexual development across the Apicomplexa. *Eukaryot Cell*. 2008
- Frenal K, Polonais V, Marq JB, Stratmann R, Limenitakis J, Soldati-Favre D. Functional dissection of the apicomplexan glideosome molecular architecture. *Cell Host Microbe*. 2010; 8(4):343–57. [PubMed: 20951968]

- Fung C, Beck JR, Robertson SD, Gubbels MJ, Bradley PJ. Toxoplasma ISP4 is a central IMC sub-compartment protein whose localization depends on palmitoylation but not myristoylation. *Mol Biochem Parasitol*. 2012
- Gajria B, Bahl A, Brestelli J, Dommer J, Fischer S, Gao X, Heiges M, Iodice J, Kissinger JC, Mackey AJ, et al. ToxoDB: an integrated Toxoplasma gondii database resource. *Nucleic Acids Res*. 2008; 36(Database issue):D553–6. [PubMed: 18003657]
- Ganter M, Schuler H, Matuschewski K. Vital role for the Plasmodium actin capping protein (CP) beta-subunit in motility of malaria sporozoites. *Mol Microbiol*. 2009; 74(6):1356–67. [PubMed: 19682250]
- Gaskins E, Gilk S, DeVore N, Mann T, Ward G, Beckers C. Identification of the membrane receptor of a class XIV myosin in Toxoplasma gondii. *J Cell Biol*. 2004; 165(3):383–93. [PubMed: 15123738]
- Gilk SD, Gaskins E, Ward GE, Beckers CJ. GAP45 phosphorylation controls assembly of the Toxoplasma myosin XIV complex. *Eukaryot Cell*. 2009; 8(2):190–6. [PubMed: 19047362]
- Gilk SD, Raviv Y, Hu K, Murray JM, Beckers CJ, Ward GE. Identification of PhIL1, a novel cytoskeletal protein of the Toxoplasma gondii pellicle, through photosensitized labeling with 5-[125I]iodonaphthalene-1-azide. *Eukaryot Cell*. 2006; 5(10):1622–34. [PubMed: 17030994]
- Goujon M, McWilliam H, Li W, Valentin F, Squizzato S, Paern J, Lopez R. A new bioinformatics analysis tools framework at EMBL-EBI. *Nucleic Acids Res*. 2010; 38(Web Server issue):W695–9. [PubMed: 20439314]
- Gould SB, Kraft LG, van Dooren GG, Goodman CD, Ford KL, Cassin AM, Bacic A, McFadden GI, Waller RF. Ciliate pellicular proteome identifies novel protein families with characteristic repeat motifs that are common to Alveolates. *Mol Biol Evol*. 2011
- Gubbels MJ, Vaishnav S, Boot N, Dubremetz JF, Striepen B. A MORN-repeat protein is a dynamic component of the Toxoplasma gondii cell division apparatus. *J Cell Sci*. 2006; 119:2236–2245. [PubMed: 16684814]
- Hakansson S, Morisaki H, Heuser J, Sibley LD. Time-lapse video microscopy of gliding motility in Toxoplasma gondii reveals a novel, biphasic mechanism of cell locomotion. *Mol Biol Cell*. 1999; 10(11):3539–47. [PubMed: 10564254]
- Heaslip AT, Dzierszynski F, Stein B, Hu K. TgMORN1 Is a Key Organizer for the Basal Complex of Toxoplasma gondii. *PLoS Pathog*. 2010; 6(2):e1000754. [PubMed: 20140195]
- Herm-Gotz A, Weiss S, Stratmann R, Fujita-Becker S, Ruff C, Meyhofer E, Soldati T, Manstein DJ, Geeves MA, Soldati D. Toxoplasma gondii myosin A and its light chain: a fast, single-headed, plus-end-directed motor. *Embo J*. 2002; 21(9):2149–58. [PubMed: 11980712]
- Hliscs M, Sattler JM, Tempel W, Artz JD, Dong A, Hui R, Matuschewski K, Schuler H. Structure and function of a G-actin sequestering protein with a vital role in malaria oocyst development inside the mosquito vector. *J Biol Chem*. 2010; 285(15):11572–83. [PubMed: 20083609]
- Hu K. Organizational changes of the daughter basal complex during the parasite replication of Toxoplasma gondii. *PLoS Pathog*. 2008; 4(1):e10. [PubMed: 18208326]
- Hu K, Johnson J, Florens L, Fraunholz M, Suravajjala S, DiLullo C, Yates J, Roos DS, Murray JM. Cytoskeletal components of an invasion machine - the apical complex of Toxoplasma gondii. *PLoS Pathog*. 2006; 2(2):121–138.
- Hubberstey AV, Mottillo EP. Cyclase-associated proteins: CAPacity for linking signal transduction and actin polymerization. *FASEB journal: official publication of the Federation of American Societies for Experimental Biology*. 2002; 16(6):487–99. [PubMed: 11919151]
- Huynh MH, Carruthers VB. Tagging of endogenous genes in a Toxoplasma gondii strain lacking Ku80. *Eukaryot Cell*. 2009; 8(4):530–9. [PubMed: 19218426]
- Johnson TM, Rajfur Z, Jacobson K, Beckers CJ. Immobilization of the type XIV myosin complex in Toxoplasma gondii. *Mol Biol Cell*. 2007; 18(8):3039–46. [PubMed: 17538016]
- Keeley A, Soldati D. The glideosome: a molecular machine powering motility and host-cell invasion by Apicomplexa. *Trends Cell Biol*. 2004; 14(10):528–32. [PubMed: 15450974]
- Keeling PJ, Burger G, Durnford DG, Lang BF, Lee RW, Pearlman RE, Roger AJ, Gray MW. The tree of eukaryotes. *Trends Ecol Evol*. 2005; 20(12):670–6. [PubMed: 16701456]

- Kono M, Herrmann S, Loughran NB, Cabrera A, Engelberg K, Lehmann C, Sinha D, Prinz B, Ruch U, Heussler V, et al. Evolution and Architecture of the Inner Membrane Complex in Asexual and Sexual Stages of the Malaria Parasite. *Molecular biology and evolution*. 2012
- Kudryashev M, Lepper S, Stanway R, Bohn S, Baumeister W, Cyrklaff M, Frischknecht F. Positioning of large organelles by a membrane-associated cytoskeleton in Plasmodium sporozoites. *Cell Microbiol*. 2010; 12(3):362–71. [PubMed: 19863555]
- Larkin MA, Blackshields G, Brown NP, Chenna R, McGettigan PA, McWilliam H, Valentin F, Wallace IM, Wilm A, Lopez R, et al. Clustal W and Clustal X version 2.0. *Bioinformatics*. 2007; 23(21):2947–8. [PubMed: 17846036]
- Leander BS, Keeling PJ. Morphostasis in alveolate evolution. *trends in Ecology and Evolution*. 2003; 18(8):395–402.
- Lorestani A, Sheiner L, Yang K, Robertson SD, Sahoo N, Brooks CF, Ferguson DJ, Striepen B, Gubbels MJ. A Toxoplasma MORN1 Null Mutant Undergoes Repeated Divisions but Is Defective in Basal Assembly, Apicoplast Division and Cytokinesis. *PLoS ONE*. 2010; 5(8)
- Lupas A, Van Dyke M, Stock J. Predicting coiled coils from protein sequences. *Science*. 1991; 252(5009):1162–1164.
- Mann T, Beckers C. Characterization of the subpellicular network, a filamentous membrane skeletal component in the parasite Toxoplasma gondii. *Mol Biochem Parasitol*. 2001; 115(2):257–68. [PubMed: 11420112]
- Mehta S, Sibley LD. Toxoplasma gondii actin depolymerizing factor acts primarily to sequester G-actin. *J Biol Chem*. 2010; 285(9):6835–47. [PubMed: 20042603]
- Morrisette NS, Sibley LD. Cytoskeleton of apicomplexan parasites. *Microbiol Mol Biol Rev*. 2002; 66(1):21–38. [PubMed: 11875126]
- Nebl T, Prieto JH, Kapp E, Smith BJ, Williams MJ, Yates JR 3rd, Cowman AF, Tonkin CJ. Quantitative in vivo Analyses Reveal Calcium-dependent Phosphorylation Sites and Identifies a Novel Component of the Toxoplasma Invasion Motor Complex. *PLoS Pathog*. 2011; 7(9):e1002222. [PubMed: 21980283]
- Porchet E, Torpier G. Freeze fracture study of Toxoplasma and Sarcocystis infective stages. *Z Parasitenkd*. 1977; 54(2):101–24. [PubMed: 415447]
- Ren J, Wen L, Gao X, Jin C, Xue Y, Yao X. CSS-Palm 2.0: an updated software for palmitoylation sites prediction. *Protein Eng Des Sel*. 2008; 21(11):639–44. [PubMed: 18753194]
- Roos DS, Donald RG, Morrisette NS, Moulton AL. Molecular tools for genetic dissection of the protozoan parasite Toxoplasma gondii. *Methods Cell Biol*. 1994; 45:27–63. [PubMed: 7707991]
- Sahoo N, Beatty W, Heuser J, Sept D, Sibley LD. Unusual kinetic and structural properties control rapid assembly and turnover of actin in the parasite Toxoplasma gondii. *Mol Biol Cell*. 2006; 17(2):895–906. [PubMed: 16319175]
- Schuler H, Matuschewski K. Regulation of apicomplexan microfilament dynamics by a minimal set of actin-binding proteins. *Traffic*. 2006; 7(11):1433–9. [PubMed: 17010119]
- Shaw MK, Compton HL, Roos DS, Tilney LG. Microtubules, but not actin filaments, drive daughter cell budding and cell division in Toxoplasma gondii. *J Cell Sci*. 2000; 113 (Pt 7):1241–54. [PubMed: 10704375]
- Sibley LD. Intracellular parasite invasion strategies. *Science*. 2004; 304(5668):248–53. [PubMed: 15073368]
- Skillman KM, Daher W, Ma CI, Soldati-Favre D, Sibley LD. Toxoplasma gondii profilin acts primarily to sequester G-actin while formins efficiently nucleate actin filament formation in vitro. *Biochemistry*. 2012
- Skillman KM, Diraviyam K, Khan A, Tang K, Sept D, Sibley LD. Evolutionarily divergent, unstable filamentous actin is essential for gliding motility in apicomplexan parasites. *PLoS Pathog*. 2011; 7(10):e1002280. [PubMed: 21998582]
- Soldati D, Meissner M. Toxoplasma as a novel system for motility. *Curr Opin Cell Biol*. 2004; 16(1):32–40. [PubMed: 15037302]
- Striepen B, Jordan CN, Reiff S, van Dooren GG. Building the perfect parasite: cell division in apicomplexa. *PLoS Pathog*. 2007; 3(6):e78. [PubMed: 17604449]

- Tran JQ, de Leon JC, Li C, Huynh MH, Beatty W, Morrissette NS. RNG1 is a late marker of the apical polar ring in *Toxoplasma gondii*. *Cytoskeleton (Hoboken)*. 2010; 67(9):586–98. [PubMed: 20658557]
- Treeck M, Sanders JL, Elias JE, Boothroyd JC. The phosphoproteomes of *Plasmodium falciparum* and *Toxoplasma gondii* reveal unusual adaptations within and beyond the parasites' boundaries. *Cell Host Microbe*. 2011; 10(4):410–9. [PubMed: 22018241]
- Washburn MP, Wolters D, Yates JR 3rd. Large-scale analysis of the yeast proteome by multidimensional protein identification technology. *Nat Biotechnol*. 2001; 19(3):242–7. [PubMed: 11231557]
- Wong W, Skau CT, Marapana DS, Hanssen E, Taylor NL, Riglar DT, Zuccala ES, Angrisano F, Lewis H, Catimel B, et al. Minimal requirements for actin filament disassembly revealed by structural analysis of malaria parasite actin-depolymerizing factor 1. *Proc Natl Acad Sci U S A*. 2011; 108(24):9869–74. [PubMed: 21628589]
- Xiao H, El Bissati K, Verdier-Pinard P, Burd B, Zhang H, Kim K, Fiser A, Angeletti RH, Weiss LM. Post-translational modifications to *Toxoplasma gondii* alpha- and beta-tubulins include novel C-terminal methylation. *J Proteome Res*. 2010; 9(1):359–72. [PubMed: 19886702]

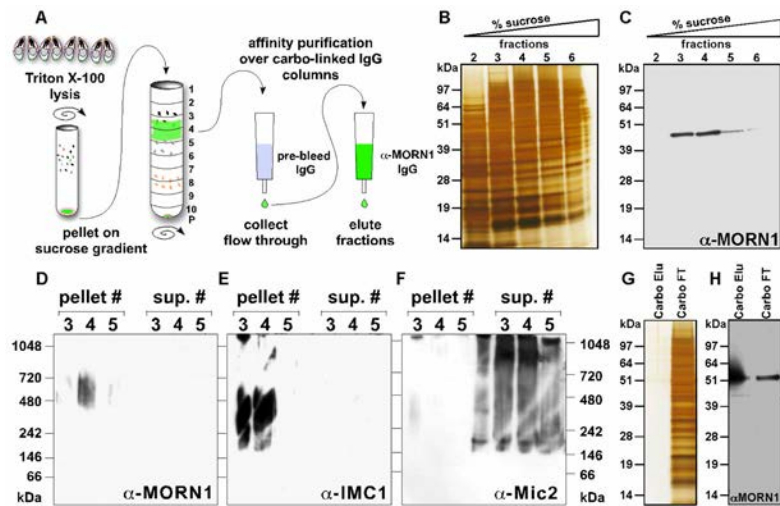


Fig. 1. MORN1 Complex Fractionation

A: Schematic of the MORN1 complex fractionation and enrichment strategy. TX-100 insoluble parasite components were fractionated in a sucrose gradient, after which the MORN1 complex enriched fractions were pre-cleared over a column packed with carbo-linked pre-immune IgG and then affinity purified over a column packed with carbo-linked anti-MORN1 IgG. **B, C:** Silver stain (B) and anti-MORN1 western blot analysis (C) of sucrose gradient fractions 2–6 separated by SDS-PAGE. **D–F:** Native blue gels separating fractions 3–5 of the pellet (TX-100 insoluble) and supernatant (TX-100 soluble) were transferred to a membrane and then probed with anti-MORN1 (D), anti-IMC1 (E), or anti-Mic2 (F). **G–H:** Silver stain (G) and western blot analysis (H) of the pre-clear column flow through (“Carbo FT”), and the affinity purification column eluate (“Carbo Elu”) separated by SDS-PAGE. The black arrowhead marks MORN1 (~41 kDa), the open arrowhead marks the IgG heavy chain (~50 kDa).

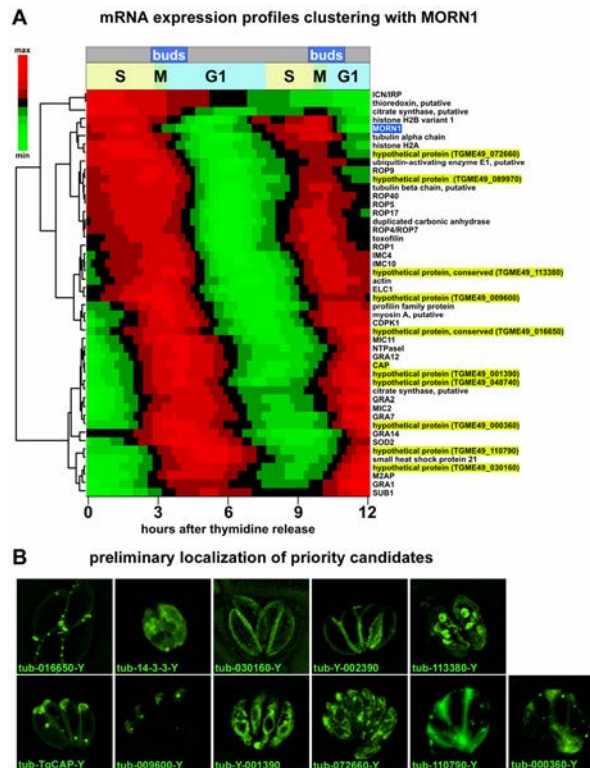


Fig. 2. mRNA expression based filter on candidate proteins identified by Mass Spectrometry
A: The available mRNA expression profiles of the proteins identified by mass spectrometry (131/137, 95.6%) were subjected to cluster analysis. The resulting dendrogram (left) included a node containing MORN1 and 47 other genes with similar mRNA expression kinetics (for complete dendrogram, see Suppl. Fig. S2). The heatmap shown to the right of the node illustrates the mRNA expression profiles of these selected genes through two cell cycles. The gene name corresponding to each row of data in the heatmap are listed at the right of the heatmap. Proteins selected for further investigation are highlighted in yellow, and MORN1 is highlighted in blue. **B:** Preliminary localization of prioritized candidates assessed by transiently overexpressing YFP-fusions in parasites and examining the living cells by fluorescence microscopy. The numbers in B correspond to TGME49 gene ID on ToxoDB. “tub” for tubulin promoter and “Y” for YFP.

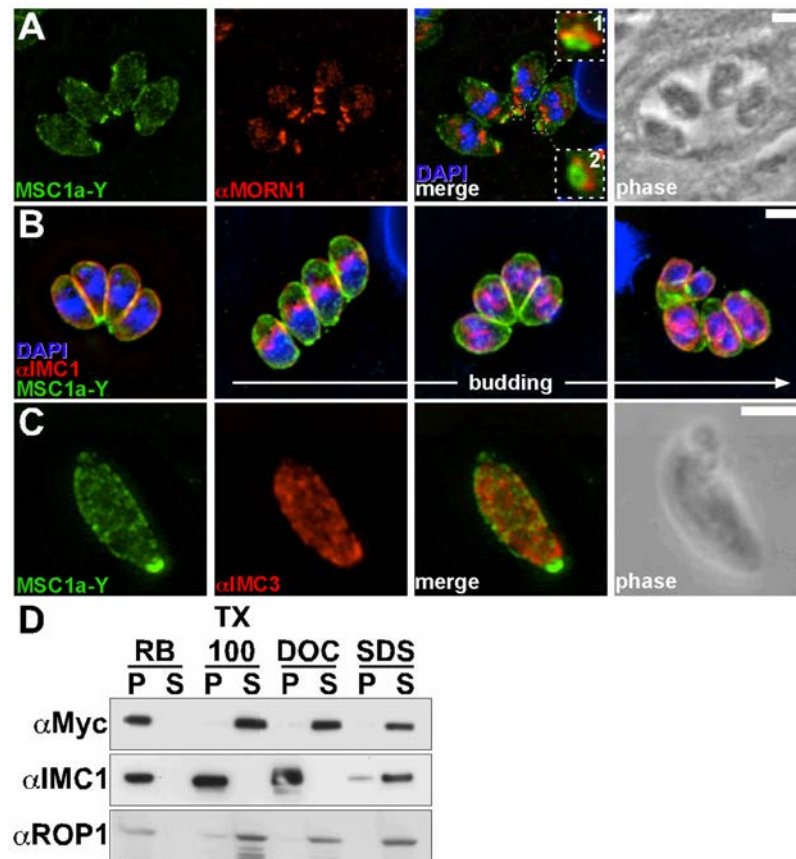


Fig. 3. TgMSC1a forms a ring in the basal complex

A–C: Parasites expressing a YFP tag fused to the 3' end of the endogenous MSC1a locus were analyzed by IFA. Intracellular parasites co-stained with anti-GFP and anti-MORN1 (A), or anti-IMC1 (B). The upper insert in (A) is a side-view of the mature basal complex, illustrating its stratified structure, and the lower insert in (A) illustrates a ring structure formed by MSC1a-YFP (green). Extracellular parasites co-stained with anti-GFP and anti-IMC3 are shown in (D). Cells shown in (A) and (C) were fixed with 100% methanol, while cells shown in (B) were fixed with 3.7% PFA and permeabilized with 0.25% TX-100. Scale bars represent 2 μ m. **D:** Differential detergent extraction analysis of MSC1a-myc3x parasites, where resuspension buffer without detergent (RB), 1% TX-100, 1% SDS or 1% DOC were used for extractions as indicated. P: pellet (insoluble fraction); S: supernatant (soluble fraction). Anti-IMC1 and anti-ROP1 hybridization were used as controls for the insoluble and soluble fraction, respectively. Image is representative of two independent experiments.

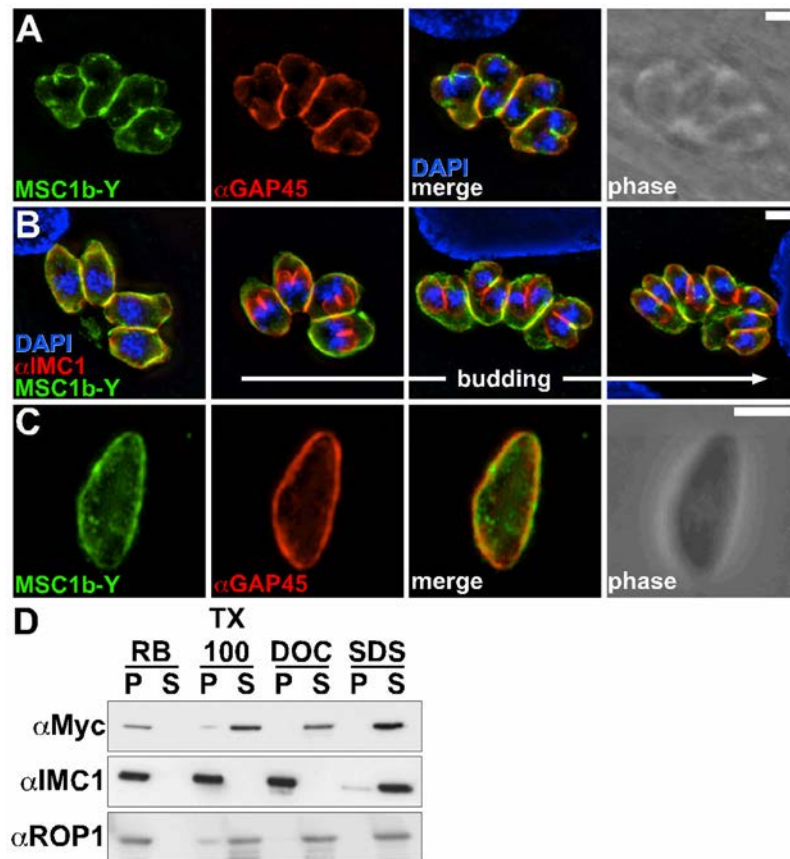


Fig. 4. TgMSC1b marks the mature IMC

A–C: Parasites expressing MSC1b-YFP fusion expressed by the endogenous promoter were analyzed by IFA. Intracellular parasites co-stained with anti-GFP and anti-GAP45 (A), or anti-IMC1 (B). Extracellular parasites co-stained with anti-GFP and anti-GAP45 are shown in (C). Cells were fixed and permeabilized with 100% methanol. Scale bars represent 2 μm .

D: Differential detergent extraction analysis of MSC1a-myc3x parasites, where resuspension buffer without detergent (RB), 1% TX-100, 1% SDS or 1% DOC were used for extractions as indicated. P: pellet (insoluble fraction); S: supernatant (soluble fraction). Anti-IMC1 and anti-ROP1 hybridization were used as controls for the insoluble and soluble fraction, respectively. Image is representative of two independent experiments.

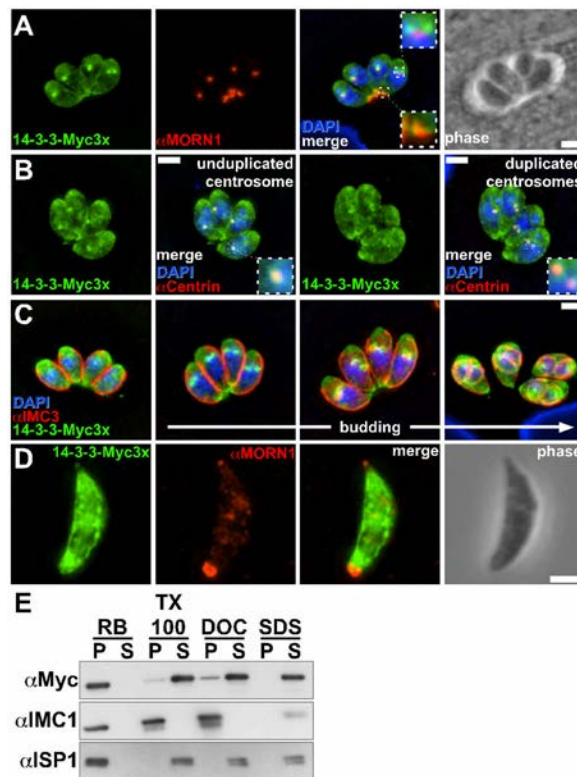


Fig. 5. Tg14-3-3 is an early marker of daughter budding

A–D: Parasites expressing three tandem Myc tags fused to the 3' end of the endogenous Tg14-3-3 locus were analyzed by IFA. Intracellular parasites co-stained with anti-myc and anti-MORN1 (A), anti-Centrin1 (B), or anti-IMC3 (C). The upper inset in (A) illustrates two Tg14-3-3 spots (green) flanking the unduplicated spindle pole (red), and the lower inset illustrates the mature basal complex. Panel C shows a sequence of different stages throughout cell division as indicated (different cells in each panel). Extracellular parasites co-stained with anti-myc and anti-MORN1 are shown in (D). Cells were fixed with 3.7% PFA and permeabilized with 0.25% TX-100. Scale bars represent 2 μ m. **E:** Differential detergent extraction analysis of Tg14-3-3-myc3x parasites, where resuspension buffer without detergent (RB), 1% TX-100, 1% SDS or 1% DOC were used for extractions as indicated. P: pellet (insoluble fraction); S: supernatant (soluble fraction). Anti-IMC1 and anti-ISP1 hybridization were used as controls for the insoluble and soluble fraction, respectively. Image is representative of two independent experiments.

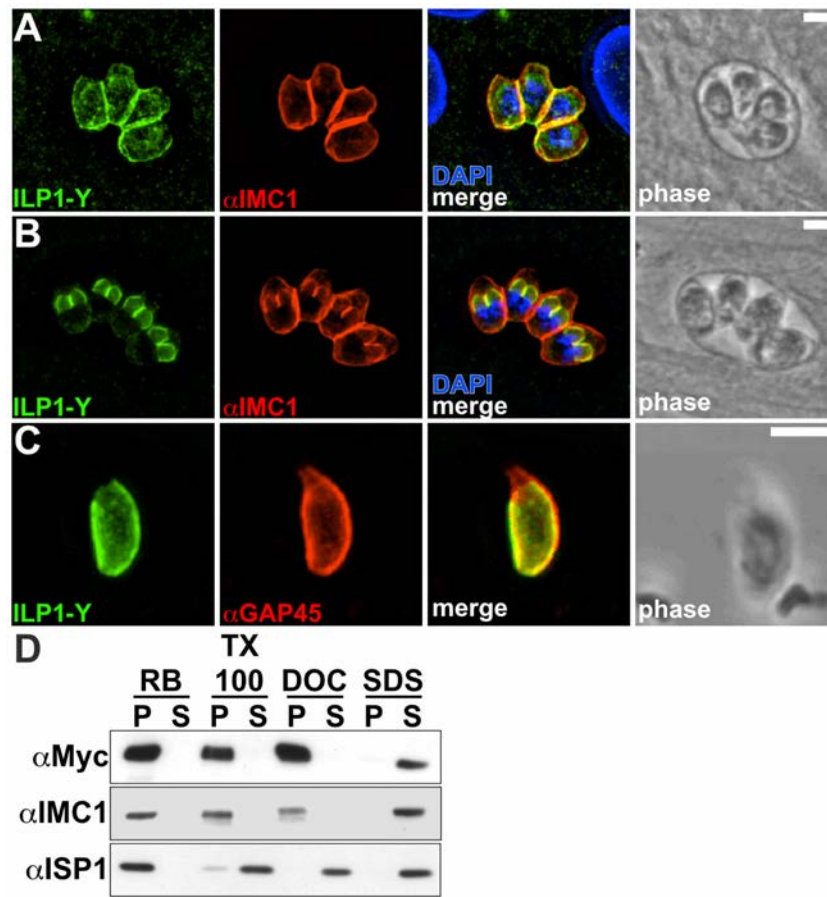


Fig. 6. TgILP1 is enriched in the daughter buds

A–C: Parasites stably expressing TgILP1-YFP whose expression was driven by the endogenous promoter were analyzed by IFA. Intracellular parasites co-stained with anti-GFP and anti-IMC1, either in interphase (A) or in cell division (B). C. Extracellular parasites co-stained with anti-GFP and anti-GAP45. Cells were fixed and permeabilized with 100% methanol. Scale bars represent 2 μ m. **D:** Differential detergent extraction analysis of TgILP1-myc3x parasites where resuspension buffer without detergent (RB), 1% TX-100, 1% SDS or 1% DOC were used for extractions as indicated. P: pellet (insoluble fraction); S: supernatant (soluble fraction). Anti-IMC1 and anti-ISP1 hybridization were used as controls for the insoluble and soluble fraction, respectively. Image is representative of two independent experiments.

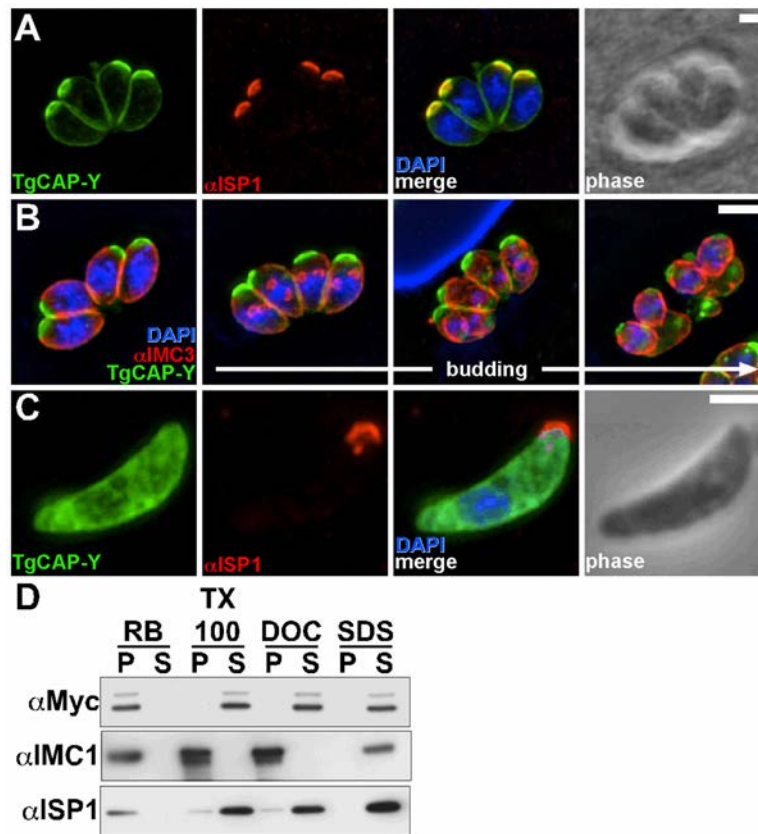


Fig. 7. TgCAP is concentrated in the apical cap of intracellular tachyzoites

A–C: Parasites stably expressing a TgCAP-YFP fusion whose expression was driven by the endogenous promoter were analyzed by IFA. Intracellular parasites co-stained with anti-GFP and anti-ISP1 (A), or anti-IMC3 (B). Panel B shows a sequence of different stages throughout cell division as indicated (different cells in each panel). C. Extracellular parasites co-stained with anti-GFP and anti-IMC3. Cells were fixed with 3.7% PFA and permeabilized with 0.25% TX-100. Scale bars represent 2 μ m. **D:** Differential detergent extraction analysis of TgCAP-myc3x parasites, where resuspension buffer without detergent (RB), 1% TX-100, 1% SDS or 1% DOC were used for extractions as indicated. P: pellet (insoluble fraction); S: supernatant (soluble fraction). Anti-IMC1 and anti-ISP1 hybridization were used as controls for the insoluble and soluble fraction, respectively. Image is representative of two independent experiments.

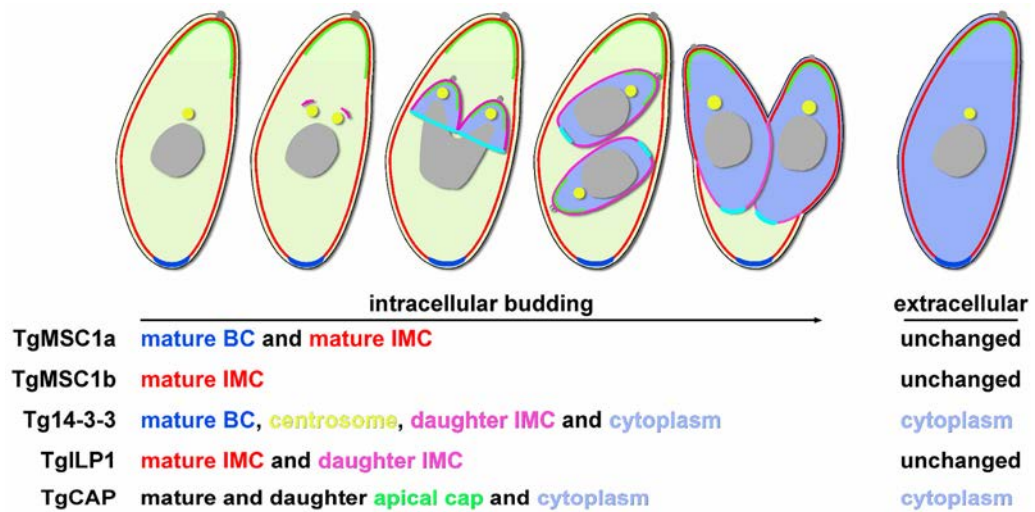


Fig 8. Schematic summary of the localization of the newly identified cytoskeletal components throughout the lytic cycle

Mature IMC is shown in red, daughter IMC is shown in magenta, centrosomes are shown in bright yellow, nucleus is shown in gray, mature basal cup is shown in dark blue, daughter basal cup is shown in light blue, apical cap is shown in bright green, the cytoplasm is shown in both light green (mother) and lavender (daughter), and the plasma membrane is shown as a thin black line surrounding the parasite.

Table 1

Candidates selected by filtering strategy

Prioritized MORN1-Interacting Candidates.

Gene ID	Descriptive Name	Prioritized Candidates		
		Preliminary Localization	Homology	Predicted Domains
TGME49_030160	hypothetical protein	IMC	<i>N. caninum</i> , <i>Plasmodium</i> spp.	RNA recognition motif
TGME49_110790	hypothetical protein	dense granules, PV lumen	<i>N. caninum</i>	signal peptide
TGME49_000360	hypothetical protein	dense granules, PV lumen	<i>N. caninum</i>	signal peptide; low complexity region
TGME49_048740	hypothetical protein	unable to PCR	<i>N. caninum</i> , <i>Micromonas</i> spp., <i>Clostridium perfringens</i> , <i>Trichomonas vaginalis</i>	coiled coil; low complexity; internal repeat 1
TGME49_001390	hypothetical protein	ER	none	signal peptide; low complexity; and transmembrane segment
TGME49_110030	adenylyl cyclase associated protein	apical cap, cytoplasmic vesicle	Eukaryotes	CARP
TGME49_016650	hypothetical protein, conserved	basal cup, apical ring, cortical	<i>N. caninum</i> , <i>Plasmodium</i> spp.	none
TGME49_002390*	hypothetical protein	mature IMC	<i>N. caninum</i> , <i>Plasmodium</i> spp.	low complexity
TGME49_009600	hypothetical protein	apical cap, cytoplasmic vesicle	<i>N. caninum</i>	low complexity
TGME49_113380	hypothetical protein, conserved	IMC	<i>N. caninum</i> , <i>Plasmodium</i> spp., <i>Cryptosporidium</i> spp., <i>Theileria</i> spp.	coiled coil; low complexity
TGME49_089970	hypothetical protein	unable to PCR	<i>N. caninum</i>	low complexity
TGME49_072660	hypothetical protein	ER	<i>N. caninum</i>	signal peptide; low complexity
TGME49_063090#	14-3-3 protein, putative	basal cup, daughter IMC, cytoplasmic vesicle cytoplasm	Eukaryotes	low complexity; 14-3-3 domain

* paralog of TGME49_016650 identified by BLAST; not identified by MudPIT

mRNA expression profile did not cluster with MORN1

Homology predicted using OrthoMCL and domains predicted using SMART sequence analysis.